

Finite-Element Analysis of the Frequency Response of a Metallic Cantilever Coupled With a Piezoelectric Transducer

Luca Dalessandro, *Student Member, IEEE*, and Daniele Rosato, *Student Member, IEEE*

Abstract—This paper is devoted to modeling the dynamic response of an electromechanical system consisting of a piezoelectric transducer glued on part of the upper surface of a metallic cantilever. The piezo works both as vibration sensor and as actuator, and the system is the basis of many vibration-control devices of current interest. A three-dimensional (3-D) finite-element method (FEM) model that reproduces the physical system is proposed, and its advantages with respect to an analytical approach and to one-dimensional (1-D) and two-dimensional (2-D) FEM models are discussed. In sensor mode, the frequency response in terms of the voltage at the electrodes is drawn; while in actuator mode, the frequency response of acceleration and displacement at the free end of the cantilever is calculated. The 3-D model has been verified through the comparison with the results from the experiment carried out at the University of L'Aquila, Italy. Furthermore, experimental inaccessible quantities such as stresses at the piezo-cantilever interface are computed in both modes as a preliminary step in the study of delamination phenomena and their impact on the performance of the system in vibration-control applications.

Index Terms—Debonding, electromechanical system three-dimensional (3-D) modeling, finite elements, frequency analysis, piezoelectric transducer.

I. INTRODUCTION

PIEZOELECTRIC materials possess intrinsic electromechanical coupling effects, by virtue of which they have found extensive applications in smart devices such as electromechanical actuators and transducers. They are largely used in active vibration control and noise suppression of sensors in structures of different scale: rockets, weapon systems, smart skin systems of submarines, and so on [1]–[3]. Piezoelectric plates appropriately assembled with structural elements can make up proper micromachines, for instance microelectromechanical systems (MEMS) or microsystems technology (MST), that have applications ranging from recent technologies of biomedical engineering to silicon technology [4]–[7]. Adhesive bonding of two piezoelectric bars (with one

of them transversally and the other longitudinally polarized) allows one to realize an alternating voltage transformer, which has good features to work for high voltages and low currents. These are the fundamental requirements to supply devices such as cathode ray tubes (CRTs) or particle accelerators.

In these applications, where piezoelectric devices are glued to the oscillating support, it is often necessary to assess experimentally inaccessible quantities, such as interlaminar mechanical stresses, electric potential, and field within the material, the knowledge of which is crucial to optimize the performance of the device and in order to assure correct working of the system. Sun *et al.* [8], Holnicki-Szulc, and Marzec [9] address the technological problem of debonding, i.e., the disjunction of the piezoelectric lamina from the host structure. Debonding compromises the system's working capacity and can decrease the efficiency of the control and measurement apparatus. Since the typical dimension of debonding phenomena is of micrometers or tens of micrometers in magnitude, a pointwise knowledge of interfacial mechanical stresses is necessary. For this aim, it is opportune and highly appropriate to use the finite-element method (FEM) [10]. The analytical solution of the differential equations providing the fields at the interface can be easily made for a one-dimensional (1-D) model of the system [11], [12], or for simple geometries [3], [13], but is very complicated for higher dimensional models and for complex geometry. However, only the resultant forces and deformations can be calculated through an analytical approach, and this does not provide any information on the points of the structure that are highly stressed. Moreover, if the coupling between longitudinal, flexural, and torsional modes is not included through a 3-D model [14], by adopting instead only a 1-D or two-dimensional (2-D) model, then the quantities calculated present large errors [10], [15]. For instance, under the assumption of a 1-D model, the interlaminar tangential stresses, which are the main stresses responsible for the disjunction of the two laminas, are zero. Besides the pointwise determination of the interfacial mechanical quantities, FE analysis also allows one to compute the pointwise values of the electric potential and field within the piezoelectric plate.

This paper analyzes the frequency response of the electromechanical system shown in Fig. 1, made up of a metallic cantilever on which a piezotransducer is bonded. A 3-D FE model is proposed and discussed that reproduces with high accuracy the real physical system. This model allows us to compute the interfacial mechanical stresses and the pointwise values of the electric potential and field within the piezoelectric plate, all of

Manuscript received August 26, 2004; revised May 5, 2005. This work was supported by the Max Planck Society, Germany.

L. Dalessandro was with the Max Planck Institute for Mathematics in the Sciences, D-04103 Leipzig, Germany. He is now with the Power Electronic Systems Laboratory, Swiss Federal Institute of Technology (ETH) Zurich, CH-8092 Zurich, Switzerland (e-mail: dalessandro@lem.ee.ethz.ch).

D. Rosato was with the Max Planck Institute for Mathematics in the Sciences, D-04103 Leipzig, Germany. He is now with the Electrical and Electronic Engineering Department (DEE), Politecnico di Bari, I-70125 Bari, Italy, and is also with the Institute of Applied Mechanics, University of Stuttgart, D-70500 Stuttgart, Germany (e-mail: rosato@mechbau.uni-stuttgart.de).

Digital Object Identifier 10.1109/TIM.2005.853677

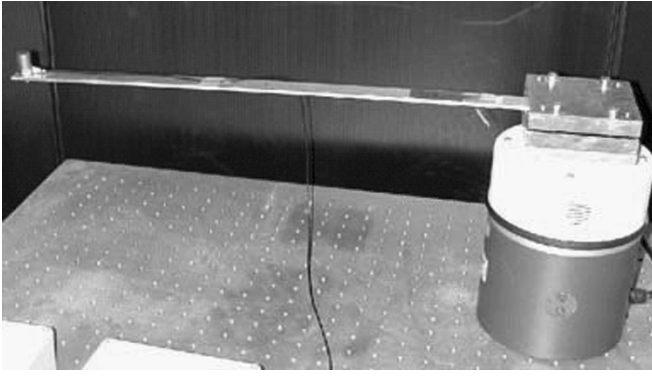


Fig. 1. Electromechanical system studied, made out of a metallic cantilever clamped at one end by a cylindrical oscillator, and of a piezoelectric transducer glued on part of the cantilever upper surface.

which are quantities that can not be derived through an analytical model or by an experiment. This model is also able to take into account the coupling between the bending, normal, and torsional vibration modes of the metallic cantilever induced by the piezoelectric transducer. Including this coupling into the model is important since it has influence on the values of the resonance frequencies of the system and on the amplitude of the stresses and deformations. Furthermore, the proposed 3-D model provides a simple and useful tool for the control design, because it accurately reproduces the physical system with the advantage that it is easier to handle and provides a quick access to the variables of the system. These aspects are clear advantages in comparison to the existing 1-D and 2-D models.

The frequency analysis is extended up to several kilohertz; this band includes the first resonance peaks. These are the most interesting for practical applications because of their higher amplitude values that are very unfavorable. This particular system is chosen because information about the frequency behavior was already available, as the system had already been studied in the course of an experiment carried out at the Dynamics Lab of the University of L'Aquila, Italy. The setup has been used in order to study structural vibrations and to control them via piezotransducers, and the debonding of the piezo from the cantilever has been observed during the tests.

For this reason, it is interesting to compare the results of the present work with experimental ones [11], in order to verify the validity and correctness of the model and then go ahead with the FE calculation of the fields at the interface. The considered system is not miniaturized, but it is the prototype of those used on a different scale for the most disparate applications. For example, a cantilever with a length of some hundreds of micrometers that hosts an integrated piezoelectric actuator/sensor can be used for extremely sensitive measurements in a wide variety of signal domains, including electrical, thermal, chemical, and magnetic. The analysis of the quantities necessary to describe and predict the behavior of the electromechanical system studied herein can be extended to similar systems but on a microscopic scale, where the interaction between electrical and mechanical phenomena becomes stronger; the system model, however, remains the same as that suggested in this paper.

This paper is organized as follows. In Section II, the relations which model the piezotransducer are presented. Section III

contains some preliminary numerical results that confirm the hypotheses of the system behavior and of the particular model proposed. Finally, in Section IV, Bode plots of the frequency response are presented and, furthermore, the interfacial mechanical stresses corresponding to the first resonance of the system are shown.

II. 3-D MODEL OF THE PIEZOELECTRIC TRANSDUCER

The piezotransducer 3-D model is completely defined by the physical laws of linear dielectrics electrostatics [16] and homogeneous solid elastodynamics [17], [18]: these laws provide differential equations that are integrated for the system's dynamic analysis, presented in Section IV. The same equations we use hereafter to model our system are presented in another form in [13]. We wish to underline the compactness and the clarity of the direct (tensor) notation used throughout, which allows an easier understanding and a faster implementation of the physical relations necessary for modeling the system. Even if the 2-D models presented in [13] and [15] show themselves to be more accurate in comparison to the 1-D models suggested in [11], [12], they do not allow the performance of any pointwise analysis on mechanical stresses and electric fields within the materials. The relations which describe the electromechanical system are presented as follows. The balance equations

$$\begin{cases} \operatorname{div} D = \rho_L \\ \operatorname{div} T + F_0 = \rho_0 \ddot{u} \end{cases} \quad (1)$$

on the body's surface become

$$\begin{cases} D \cdot n = \sigma_L \\ Tn = p \end{cases} \quad (2)$$

The kinematic constraints are

$$\begin{cases} E = -\nabla\varphi \\ S = \frac{1}{2}(\nabla u + \nabla u^T) \end{cases} \quad (3)$$

Here, E is the electric field vector, D is the electric displacement vector, φ the electric potential, and ρ_L and σ_L are the volume and surface charge densities, respectively. S represents the infinitesimal strain tensor, T is the stress tensor, u the displacement field (∇u^T is for the transpose of ∇u), n the outward unit normal to the boundary, F_0 and ρ_0 are, respectively, the body forces and the density in the reference configuration, and p represent the surface forces. The symbols ∇ and div indicate gradient and divergence. Constitutive equations should be added to the previous relations and should be formulated with the aim of taking into account the lowest coupling possible between each of the quantities of the following pairs:

$$(S, E) (S, D) (T, E) (T, D).$$

If S and E are chosen as independent variables, constitutive relations assume the following form:

$$\begin{cases} T = c^E S - eE \\ D = e^T S + \varepsilon^S E \end{cases} \quad (4)$$

where c^E is the tensor of rank four of the elastic constants holding as constant the electric field E , ε^S is the tensor of rank two of the dielectric permittivities for constant S , and e

(e^T being the transpose of e) is the tensor of rank three of the piezoelectric constants. Let us recall that piezoelectricity does not introduce new physical laws; the novelty is in the coupling between electrical and mechanical quantities. Generally, the piezoelectricity constitutive law is obtained by choosing an opportune thermodynamic function (function of the selected independent variables) and linearizing it around its minimum point [19], [20]. The previous relations provide the differential equations only in terms of the state variables φ and u .

By using Voigt notation, which allows to convert a tensorial formulation into a matrix form [21], [22], the piezoelectric constitutive equations (4) assume the form we have implemented and used for the FEM analysis

$$\begin{aligned} \begin{bmatrix} \sigma_1 \\ \sigma_2 \\ \sigma_3 \\ \sigma_4 \\ \sigma_5 \\ \sigma_6 \end{bmatrix} &= \begin{bmatrix} c_{11} & c_{12} & c_{13} & 0 & 0 & 0 \\ c_{12} & c_{22} & c_{23} & 0 & 0 & 0 \\ c_{13} & c_{23} & c_{33} & 0 & 0 & 0 \\ 0 & 0 & 0 & c_{44} & 0 & 0 \\ 0 & 0 & 0 & 0 & c_{55} & 0 \\ 0 & 0 & 0 & 0 & 0 & c_{66} \end{bmatrix} \\ &\times \begin{bmatrix} \varepsilon_1 \\ \varepsilon_2 \\ \varepsilon_3 \\ \varepsilon_4 \\ \varepsilon_5 \\ \varepsilon_6 \end{bmatrix} - \begin{bmatrix} 0 & e_{12} & 0 \\ 0 & e_{22} & 0 \\ 0 & e_{12} & 0 \\ 0 & 0 & 0 \\ 0 & 0 & 0 \\ 0 & 0 & 0 \end{bmatrix} \begin{bmatrix} E_1 \\ E_2 \\ E_3 \end{bmatrix} \\ \begin{bmatrix} D_1 \\ D_2 \\ D_3 \end{bmatrix} &= \begin{bmatrix} 0 & 0 & 0 & 0 & 0 & 0 \\ e_{12} & e_{22} & e_{12} & 0 & 0 & 0 \\ 0 & 0 & 0 & 0 & 0 & 0 \end{bmatrix} \begin{bmatrix} \varepsilon_1 \\ \varepsilon_2 \\ \varepsilon_3 \\ \varepsilon_4 \\ \varepsilon_5 \\ \varepsilon_6 \end{bmatrix} \\ &+ \begin{bmatrix} \varepsilon_1^S & 0 & 0 \\ 0 & \varepsilon_2^S & 0 \\ 0 & 0 & \varepsilon_3^S \end{bmatrix} \begin{bmatrix} E_1 \\ E_2 \\ E_3 \end{bmatrix} \end{aligned} \quad (5)$$

The parameters e_{ij} ($i = 1, 2; j = 2$) in (5) are called piezoelectric stress coefficients and represent the ratio between the mechanical stress applied to the piezoelectric plate in direction x_i ($x_i, i = 1, 2, 3$ represents the unit vector of the reference coordinate frame) and the electric field along x_j , or equivalently, the ratio between the charge on the electrodes and the mechanical strain (dimensionally N/Vm). One can prove that the matrix of elastic constants c_{ij} , the matrix of piezoelectric coefficients e_{ij} and matrix of permittivities ε_i^S assume the structure shown in (5) in the case of transverse isotropy. The dielectric losses are ignored so that the dielectric permittivity matrix turns out with real coefficients. Such an assumption is admissible considering the frequency range [0–1000] Hz to which the frequency analysis is extended. The elastic constant matrix also possesses real coefficients, but the mechanical losses are taken into account by damping coefficients. If one assumes that the piezoelectric solid is isotropic, the coefficients of matrix c^E are given by

$$\begin{aligned} c_{11} = c_{22} = c_{33} &= \frac{(1-\nu)}{(1+\nu)(1-2\nu)} E \\ c_{12} = c_{13} = c_{23} &= \frac{2\nu G}{(1-2\nu)} \\ c_{44} = c_{55} = c_{66} &= G \end{aligned} \quad (6)$$

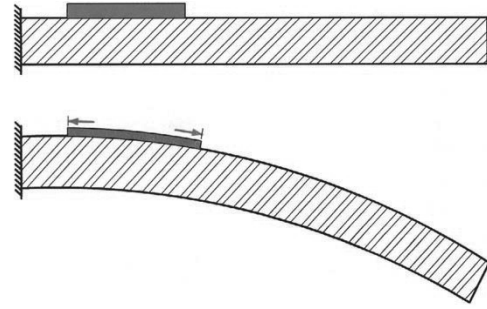


Fig. 2. Effect of the piezoactuator extension on the metallic cantilever due to the applied voltage.

where E is Young's modulus, G shear modulus, and ν Poisson's ratio.

In the actuator function, the stress acting on the piezoelectric plate due to the effect of the applied electric field, gives rise to expansions and contractions of the plate along the x_1 direction (cf. Fig. 3). Moreover, since the actuator is glued to the metallic cantilever, this latter transfers axial (flexural) stresses every time it bends because of the actuator's action (cf. Fig. 6 in [12]). The oscillating cantilever also transfers axial stresses to the piezoplate operating in the sensor mode. Therefore, the piezoplate is loaded by an eccentric axial force, to which an axial stress state corresponds. In our analysis, we assume a plane stress state and x_3 as the principal direction perpendicular to the principal plane $x_1 - x_2$, which is stress free (cf. Fig. 4).

For the sake of completeness, let us observe that the cantilever beam model is traced back to the generalized form of Hooke's Law and to the motion equation already introduced for the piezoelectric plate. Table I shows the values of geometrical and material parameters we adopt, chosen to match the existing experimental setup [11], [23].

III. PRELIMINARY TESTS ON PIEZOELECTRIC PLATE, CANTILEVER BEAM, AND COUPLED SYSTEM

Before the frequency analysis, preliminary tests were carried out on the system model that consider the metallic cantilever beam separately from the piezoelectric lamina. The aim of these tests is to confirm the assumptions on the mechanical behavior of the system and to verify the assignment of material parameters made by matrices of a particular structure as introduced in the previous section. We implement FE models of the piezoelectric transducer, of the metallic cantilever, and of the coupled system using plane stress elements. Computations are performed by implementing the user-defined models and boundary conditions in the finite element software package ABAQUS.

At first, we verify the longitudinal functioning of the piezoactuator, which by shrinking and expanding, stretches the cantilever upper fibers to which it is glued, thus making it oscillate as shown in Fig. 2. The piezoactuator is modeled assigning the mechanical, dielectric, and piezoelectric properties through (5) and, moreover, using the same geometry of the device present in the electromechanical system of the experiment. The lower basis and the left edge of the piezoplate are bonded with sliding bearings in order to allow dilatations along the horizontal and vertical directions. The lower electrode potential is set as zero,

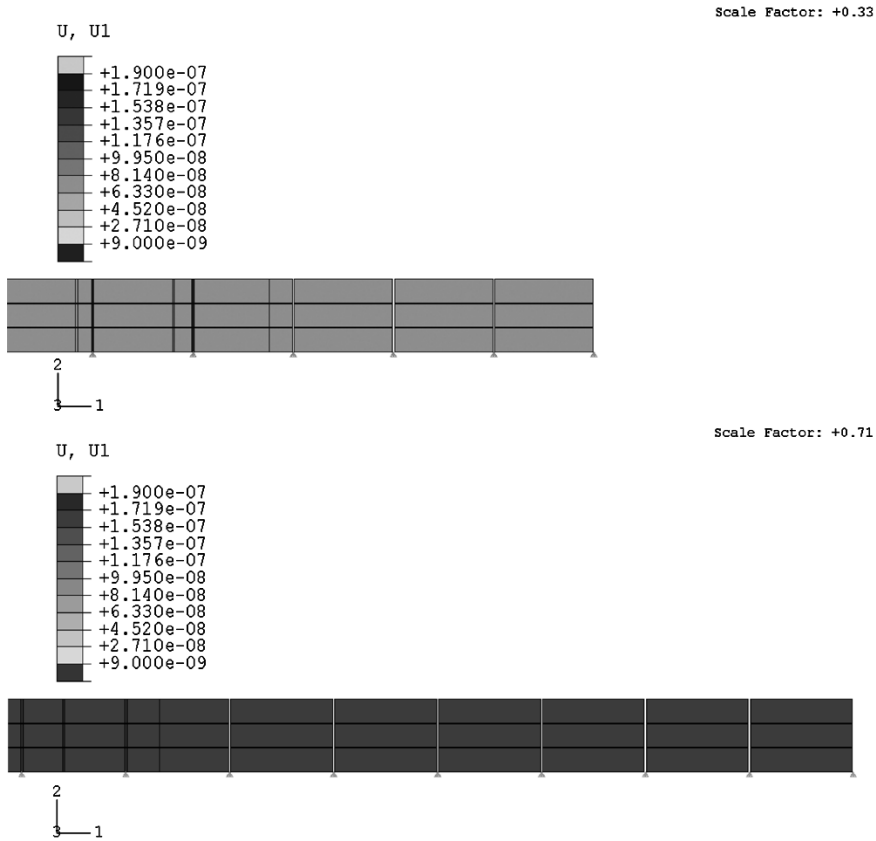


Fig. 3. Two snapshots showing the longitudinal vibrations of the piezoactuator induced by applying an alternating voltage across the lamina. In particular, the sliding bearings fixed to the lower basis allow the lamina's displacement along x_1 .

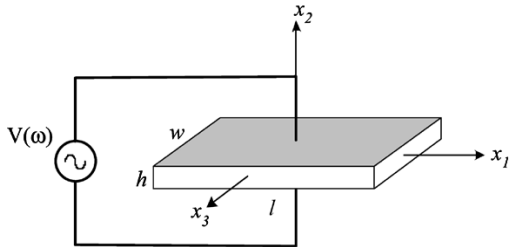


Fig. 4. Sketch of the piezoelectric plate.

and the upper one is assigned an alternating voltage of 100 V. By this numerical simulation, two snapshots of which are shown in Fig. 3, the desired longitudinal vibrations are verified instead of the thickness oscillations.

We have verified with a similar approach the presence of a voltage across the piezoelectric plate working in sensor mode, which is due to vibrations of the cantilever oscillating with acceleration at its clamped end of 1 m/s^2 in magnitude.

Afterwards, the system's natural frequencies have been extracted to perform a first comparison with the experimental values and to have a first assessment of the flexural modes occurring in the frequency band of the analysis. The piezoelectric lamina was first considered separately from the metallic one.

The piezotransducer with an alternating voltage of pulsation ω applied across its upper and lower surfaces is shown in Fig. 4. The electric current is provided by

$$I = j\omega \int_{\Sigma} D_2 dx_1 dx_3 \quad (7)$$

TABLE I
MECHANICAL AND ELECTRICAL CHARACTERISTICS OF MATERIALS

	CANTILEVER	PIEZO
Material	Aluminium	PZT
Size	$\ell_c = 510 \text{ mm}$ $w_c = 25.4 \text{ mm}$	$\ell = 50.8 \text{ mm}$ $w = 25.4 \text{ mm}$
Height	$h_c = 3.175 \text{ mm}$	$h = 0.381 \text{ mm}$
Density	$\rho_A = 2773 \text{ kg/m}^3$	$\rho = 7700 \text{ kg/m}^3$
Young's modulus	$E_A = 6.77 \cdot 10^{10} \text{ N/m}^2$	$E = 6.9 \cdot 10^{10} \text{ N/m}^2$
Poisson's ratio	$\nu_A = 0.3$	$\nu = 0.3$
Piezoelectric strain coefficients	—	$d_{12} = -179 \cdot 10^{-12} \text{ m/V}$ $d_{22} = 350 \cdot 10^{-12} \text{ m/V}$
Dielectric Permittivity	—	$\epsilon^S = 1.59 \cdot 10^{-8} \text{ F/m}$
Moment of Inertia along x_1	$J_1 = 6.77 \cdot 10^{-11} \text{ m}^4$	—

where Σ indicates the electrode surface, j is the imaginary unit, and D_2 is the component of D along x_2 . The admittance can be calculated as the ratio of the current and the voltage across the plate [19], and its value is given by

$$Y = j\omega C_0 \left(1 + \frac{k_{12}^2}{1 - k_{12}^2} \frac{\text{tg}\zeta}{\zeta} \right) \quad (8)$$

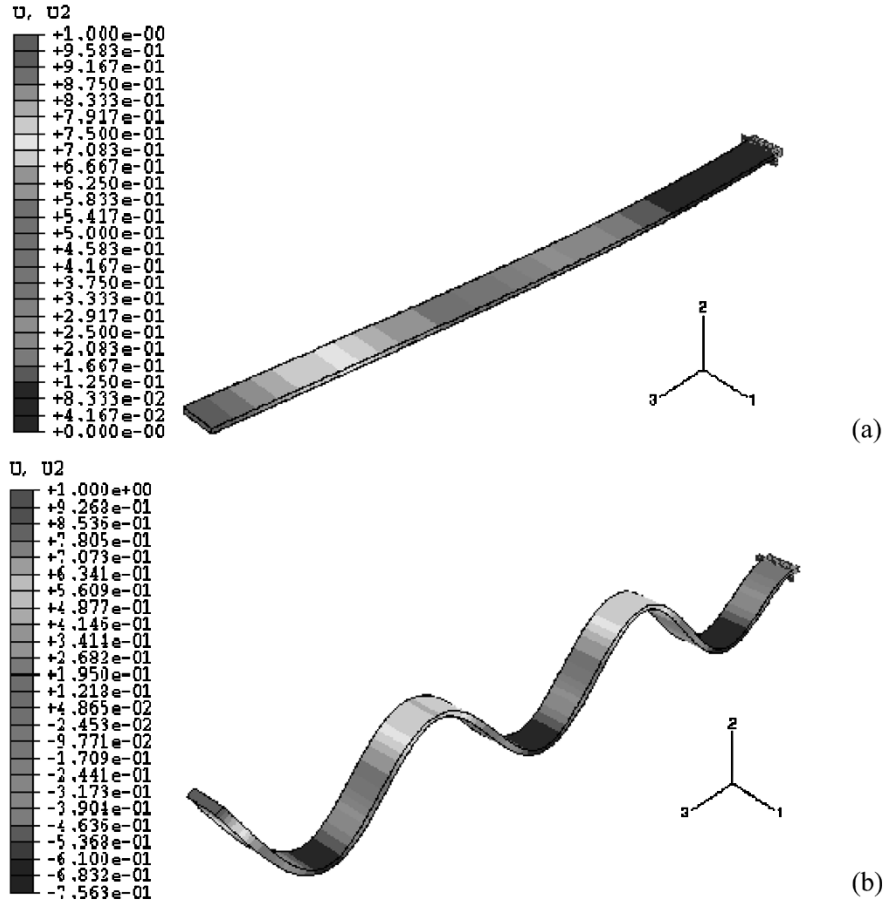


Fig. 5. Shape functions corresponding to (a) the first and to (b) the sixth flexural oscillating mode. The legend indicates the value of the displacement u_2 .

where C_0 is the static capacitance ($\omega = 0$), defined as

$$C_0 = \frac{\varepsilon_2^s w \ell}{h} \quad (9)$$

where ℓ , w , and h are, respectively, the length, width, and height of the piezoelectric lamina. The electromechanical coupling coefficient k_{12} is defined as $d_{12}^2 / (\varepsilon_2^s s_1^E)$; s_1^E is the elastic susceptibility or the inverse of the elastic constant c_1^E in the direction x_1 . The coefficient d_{12} is a piezoelectric strain coefficient, defined as the ratio of the induced mechanical strain along x_1 of the piezoelectric plate and the applied electric field in direction x_2 ; $e_{12} = E d_{12}$ provides the relation between piezoelectric stress and strain coefficients. ζ is dependent on lamina characteristic parameters

$$\zeta = \frac{\omega \ell}{2} \sqrt{\frac{\rho}{c_1^E}} \quad (10)$$

The resonance and antiresonance conditions are

$$\begin{aligned} Y \rightarrow \infty \quad \text{tg} \zeta \rightarrow \infty \quad (\text{shortcircuit}) \\ Y \rightarrow 0 \quad 1 + \frac{k_{12}^2}{1 - k_{12}^2} \frac{\text{tg} \zeta}{\zeta} = 0 \quad (\text{open circuit}) \end{aligned}$$

In particular, resonance frequencies are provided by

$$f_n = \frac{(2n - 1)}{2\ell} \sqrt{\frac{c_1^E}{\rho}} \quad (11)$$

By substituting $n = 1$, the formula (11) yields $f_1 = 29.5$ kHz, which is the first resonance frequency of the piezoelectric plate. This value is much larger than the resonance frequency of the metallic beam, and outside the frequency band of interest for our analysis. This was foreseen because the metallic cantilever possesses dimensions ten times larger than those of the piezoelectric lamina. The dependence of the frequency value on the mass is expressed in (13). It is important to note that the previous analysis is independent of the working mode of the piezoelectric plate.

On the other hand, theoretical values of natural frequencies of the metallic cantilever can only be determined through the motion equation

$$\frac{E_A}{2(1 + \nu_A)} \Delta u + \frac{E_A}{2(1 + \nu_A)(1 - 2\nu_A)} \nabla \text{div} u + F_A = \rho_A \ddot{u} \quad (12)$$

in the unknown displacement $u(x, t)$. F_A and ρ_A are, respectively, the body forces and density of the metallic cantilever in the reference configuration, and E_A and ν_A are Young's modulus and Poisson's ratio for aluminum. The solution of (12) for the case of pure bending in the $x_2 - x_3$ plane (cf. Fig. 5), provides the theoretical values of the natural frequencies

$$f_i^{23} = \frac{k_i}{2\pi} \sqrt{\frac{E_A J_1}{m_c \ell_c^3}} \quad (13)$$

TABLE II
NATURAL FREQUENCIES OF THE METALLIC CANTILEVER

<i>i</i> - Mode	k_i	f_i^{23} [Hz] theoretical	f_i^{23} [Hz] FE calculated
1	3.5156	9.740	9.746
2	22.033	61.04	61.06
3	61.701	170.9	170.9
4	120.91	334.9	334.8
5	199.85	553.6	553.2
6	298.56	827.0	826.0

where the superscript 23 indicates that the oscillations occur in the x_2-x_3 plane, m_c and ℓ_c are the cantilever's mass and length, and J_1 the cantilever moment of inertia along x_1 . By substituting the values of the constant k_i related to the first six flexural modes, it turns out that the calculated frequencies f_i^{23} are in perfect agreement with the values computed through the FE model, as shown in Table II. Fig. 5 shows the shape functions corresponding to the first and sixth flexural oscillating mode. Since (12) is derived from the 3-D expressions (1)–(3), it allows calculation of the resonance frequencies corresponding to torsional modes. The first torsional frequency calculated for the metallic cantilever is 78 Hz, and this value is between the third and fourth flexural frequencies shown in Table II.

Finally, we consider the coupled system, including the accelerometer present in the experimental apparatus (cf. Fig. 1). For the construction of the model, the following assumptions are made.

- 1) There exists a plane stress state within the two laminas, which can be realized by using plane stress elements in the numerical simulations. In such a way, all the problem's quantities are constrained to possess only components parallel to the $x_2 - x_3$ plane (cf. Fig. 5).
- 2) The upper and lower surfaces of the piezoelectric lamina are equipotential. In particular, the nodes of the lower surface have potential equal to zero and those of the upper basis, the same voltage magnitude. In the real device, such a condition is imposed by means of the electrodes.
- 3) The two laminas are perfectly glued; the system is modeled as a unique body made out of two different materials, aluminum and piezoelectric transducer (PZT), having different properties.

The accelerometer is modeled as a punctual mass kinematically constrained to the upper end of the cantilever's free basis. Such a mass is positioned at a distance of 1 cm from the center of mass of the beam-section. Mesh is realized for the sake of having the largest number of elements correspond with the interface of the piezoelectric plate and along the thickness of the two laminas, thus increasing the accuracy of the assessment of the quantities within the piezo and at the interface between the two plates.

Thereafter, natural frequencies are calculated with the presence of a concentrated mass, constituting of the accelerometer, whose weight is 0.02 kg. In such a way, the total mass of the system increases producing a decrease in the frequency values, as follows directly from (13). In Table III (second column), the

TABLE III
SYSTEM'S NATURAL FREQUENCIES [Hz]

<i>i</i> - mode	Cantilever and Accelerometer	Coupled System (Actuator Mode)	Coupled System (Actuator Mode)	Coupled System (Sensor Mode)
	FEM Computed Value	FEM Computed Value	Theoretical Value	Theoretical Value
1	7.45	7.64	7.66	7.67
2	50.94	51.19	51.89	51.90
3	148.59	149.41	150.03	150.04
4	297.58	299.17	298.96	299.13
5	497.27	505.53	499.72	500.14
6	744.41	766.73	752.54	753.06

values of natural frequencies corresponding to the system made out of the cantilever and accelerometer are presented. In the third column, the computed frequency values when the piezoelectric plate is included in the system are shown. In this last case, the cantilever's flexural strength $E_A J_1$ is increased because of the gluing of the piezoelectric lamina, hence an increase of the system's frequency values, respect of those in column two, follows.

The stiffening effect induced by the coupling of the cantilever with the piezoelectric is of two types.:

- 1) Mechanical: the gluing of the piezolamina produces an increase in the cross-sectional area and, consequently, in its moment of inertia J_1 .
- 2) Electrical: as a consequence of the electromechanical coupling, the piezoelectric plate's effective elastic tensor c^{E*} in the sensor mode (electrodes left open) is:

$$\|c^{E*}\| = \|c^E + e(\epsilon^S)^{-1}e^T\| > \|c^E\|. \quad (14)$$

If one shorts the electrodes of the piezotransducer, the stiffening effect due to the electromechanical coupling is absent (since φ and E are zero). Such a condition corresponds to the actuator mode (electrodes shorted) or when using a charge or current readout instead of a voltage readout. The frequencies presented in the third column of Table III are obtained when the actuator mode is working. During the extraction of the natural frequencies, only the mechanical stiffening has been taken into account, since the adopted FE code ignores the constraints on electric potentials for this kind of operation; the computed values, therefore, correspond to the condition of the shorted piezoelectric lamina's electrodes. In the fifth column of Table III, the frequencies of the coupled system, corresponding to the piezo working as sensor, are shown in order to highlight the previous theoretical considerations. Such values have been borrowed from [11]. From Table III, a good agreement between computed and experimental values is evident.

IV. NUMERICAL RESULTS

We have determined numerically the frequency response of the electromechanical system in terms of displacement and acceleration of the cantilever free end, corresponding to an electric

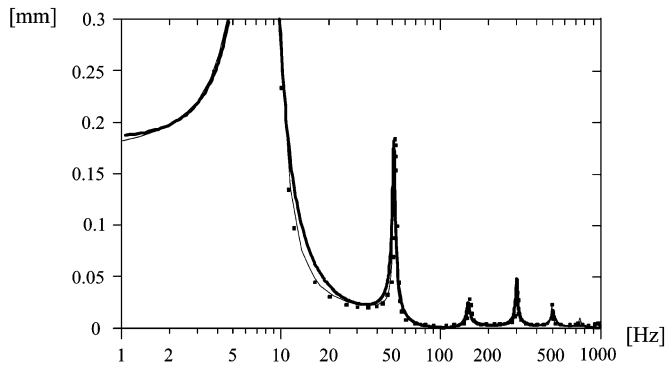


Fig. 6. Displacement magnitude of the cantilever free end corresponding to oscillations induced by the piezoactuator, in the frequency range [0–1000] Hz. Frequency responses of the proposed 3-D model (bold line), experimental values (points) and from the available 1-D analytic model (thin line, after [11]) are compared.

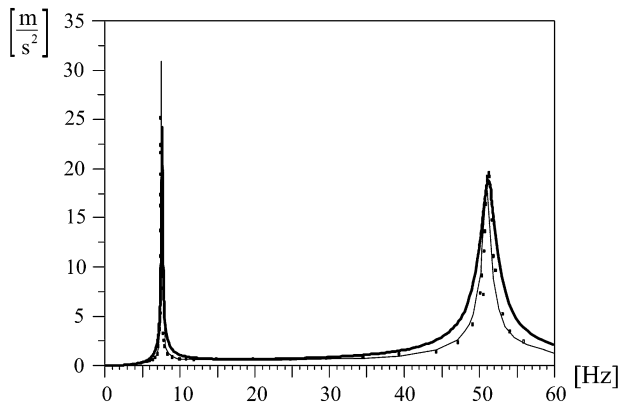


Fig. 7. Acceleration magnitude of the cantilever free end corresponding to oscillations induced by the piezoactuator, in the frequency range [0–60] Hz. Frequency responses of the proposed 3-D model (bold line), experimental values (points) and from the available 1-D analytic model (thin line, after [11]) are compared.

input represented by the alternative voltage applied across the piezoelectric plate (actuator mode). We have also computed the frequency response in terms of voltage across the electrodes of the piezoelectric plate corresponding to alternative oscillations induced by an oscillator (sensor mode). Although the extraction of the natural frequencies requires a knowledge of the mass and stiffness only, the dynamic analysis needs to take into account the dissipative forces as well as those of inertia by introducing damping coefficients. Thus, in order to compute the system frequency response obtained by a direct integration of the differential equations presented in Section II, global damping coefficients have been used in the model, and they have been determined through a least-square interpolation [25] of the modal damping coefficients available from the experiment.

Figs. 6 and 7 show, respectively, the frequency behavior of the displacement of the free end in the frequency band [0–1000] Hz and of the acceleration of the same point, in the band [0–60] Hz. In the figures, points indicate the experimental values while the bold and thin lines are calculated by the proposed 3-D FEM model and by the 1-D model [11], respectively. The frequency behavior of the voltage across the electrodes is depicted in Figs. 8 and 9, where the bands [0–30] Hz in linear scale and [30–1000] Hz in semilogarithmic scale are represented.

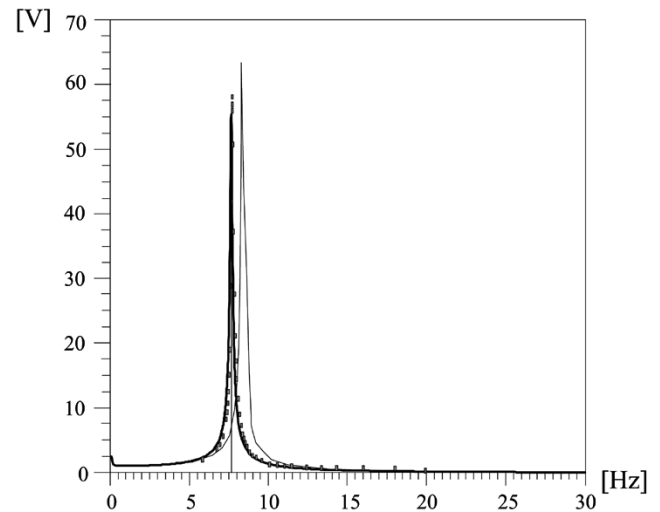


Fig. 8. Voltage magnitude across the piezoelectric sensor corresponding to oscillations induced in the cantilever beam by the oscillator, in the frequency range [0–30] Hz. Frequency responses of the proposed 3-D model (bold line), experimental values (points) and from the available 1-D analytic model (thin line, after [11]) are compared.

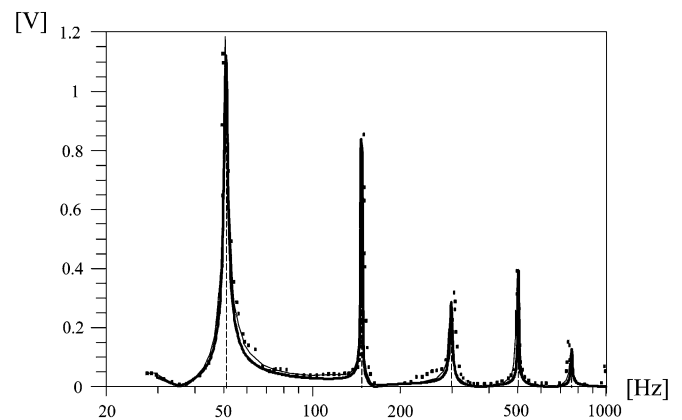


Fig. 9. Voltage magnitude across the piezoelectric sensor corresponding to oscillations induced in the cantilever beam by the oscillator, in the frequency range [30–1000] Hz. Frequency responses of the proposed 3-D model (bold line), experimental values (points) and from the available 1-D analytic model (thin line, after [11]) are compared.

The comparison with the available frequency plots [11] representing the experimental response (points) is shown: it is evident that there is agreement between the numerical results obtained by the FE model and the experimental response. The results presented have been obtained with a rectangular nonuniform grid of eight-node linear elements, which makes it possible to obtain the same quality with fewer elements (and, hence, smaller computational cost) than the others. In particular, the mesh has been taken very close in the portion of the metallic cantilever that is bonded to the piezotransducer; in such a way, the survey about the interfacial quantities, which is the goal of this work, becomes more accurate. In Figs. 11 and 12, the numerical computation of tangential stresses at the interface between the metallic cantilever and the piezotransducer are shown. The knowledge of these stress values is essential to correctly bond the piezo and to grant the device tightness during the ordinary operation in vibration. We have calculated the most unfavorable values of interfacial stresses occurring at the first resonance peak, which

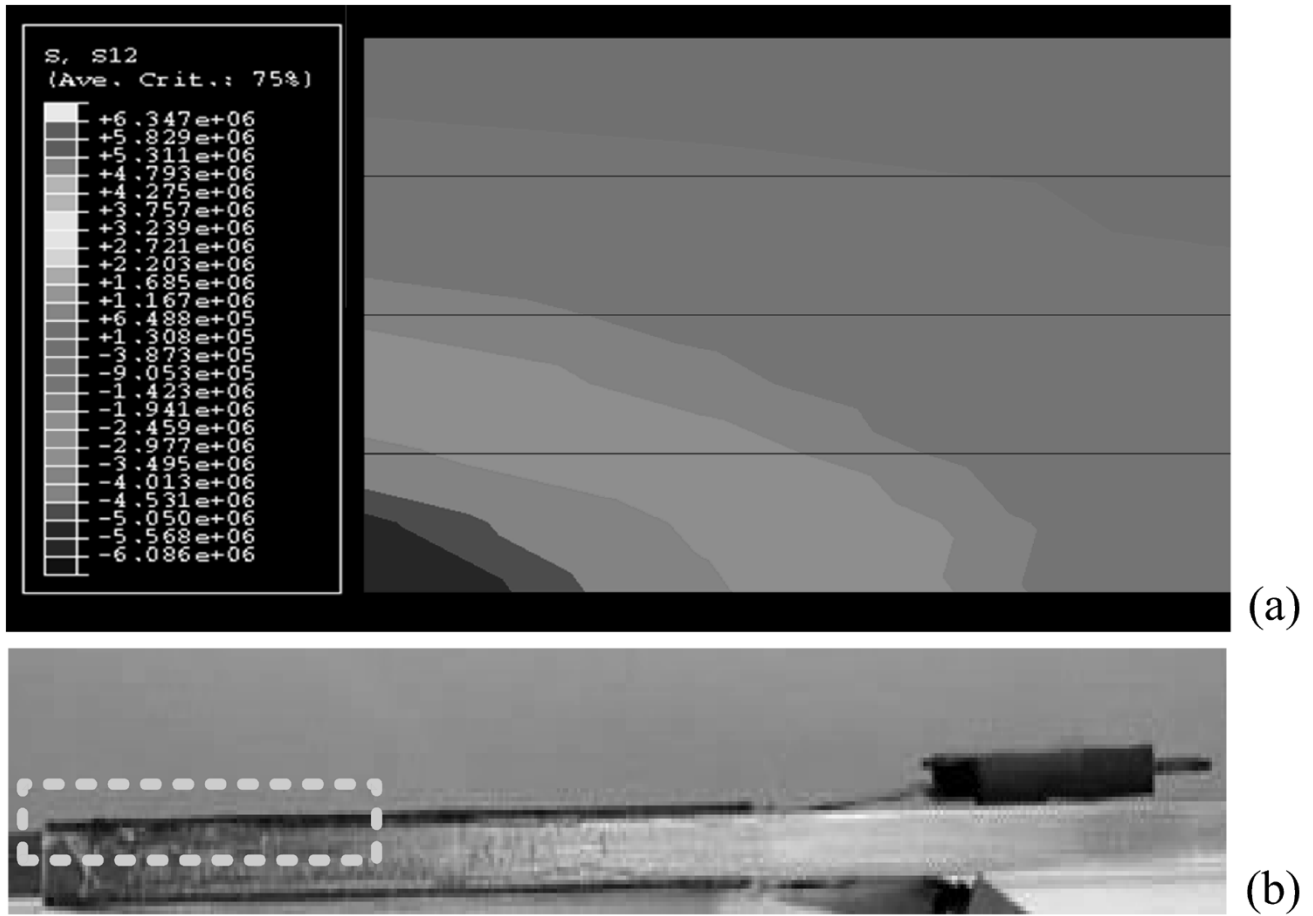


Fig. 10. FE simulation (a) shows the gathering of the tangential stresses τ_{12} at the corner of the piezoplate, which becomes the most stressed part. (b) Particular of the portion of the cantilever on which the piezotransducer is glued.

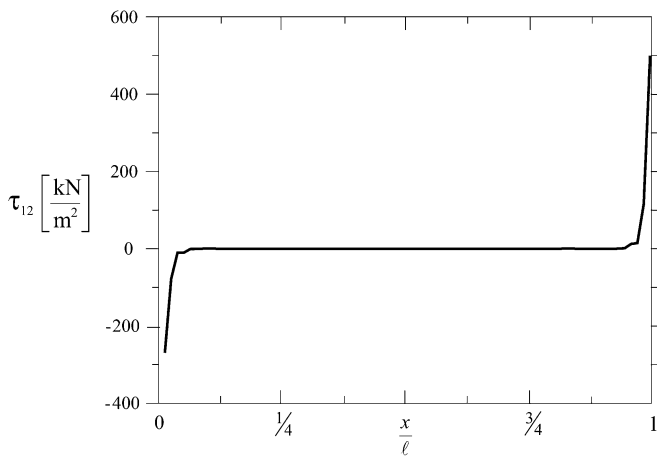


Fig. 11. Peak values of the tangential stresses τ_{12} at the piezobeam interface for the actuator mode.

falls into frequencies of about 8 Hz. Fig. 10(b) shows the portion of the electromechanical system where the piezoelectric plate is glued; the particular of the left end shows the gathering of stresses at the piezoelectric lamina's corner. Tangential stresses τ_{12} (along the x_2 direction) are diagrammed in Fig. 11, where the values represented are those assumed to correspond to the central node of each element in which the interface has been divided.

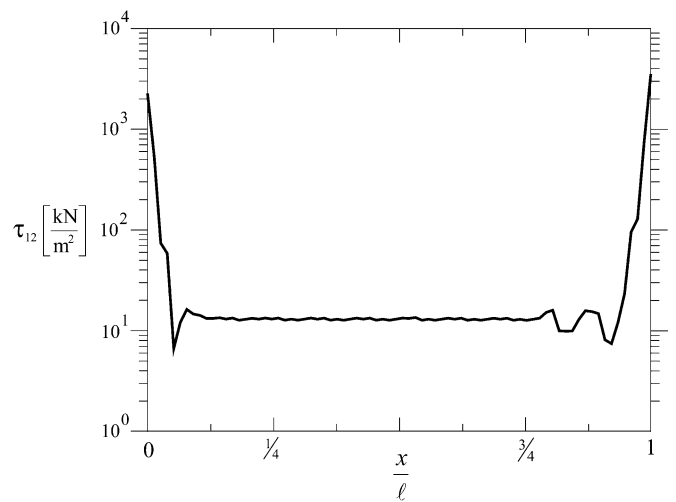


Fig. 12. Amplitude of the tangential stresses τ_{12} at the piezobeam interface for the sensor mode in semilogarithmic scale.

This diagram represents stresses τ_{12} when an alternative voltage is applied to the piezotransducer (actuator mode). Fig. 12 represents stresses τ_{12} when vibrations are induced by the shaker that makes the cantilever oscillate (sensor mode). In Fig. 13, the calculated pointwise values of the electric potential within the piezoelectric plate working as a sensor are shown. The calculation is made in correspondence to the first resonance



Fig. 13. Pointwise values of the electric potential within the piezoelectric plate; the legend indicates the potential's value (EPOT) within the materials. The field is not uniform at the left end of the piezo, since the strains are not constant and they assume the largest value in correspondence to those points.

peak, which falls into frequencies of about 8 Hz. The potential rises linearly along the height of the piezoelectric transducer, until it reaches a null value at the interface with and within the host cantilever beam. The field, however, is not uniform at the left end of the piezo, since the strains are not constant and they assume the largest value in correspondence to those points.

V. CONCLUSION

In this paper, we have numerically studied the frequency response of an electromechanical system made of a metallic cantilever hosting piezoelectric lamina working in both sensor and actuator modes. The results are in agreement with available experiments [11] and, thus, confirm the correctness and validity of our FE model. The issues shown and discussed in this paper provide the general means to realize the 3-D numerical model of an electromechanical system. Relations characterizing dielectrics, piezoelectric plates, and continuum solids have been reexamined, explaining the particular structure of matrices. In order to calculate the interfacial mechanical stresses, we have used a 3-D model that is able to take into account the coupling between longitudinal, flexural, and torsional modes, resulting in a more accurate reproduction of the physical system. By contrast, a uniaxial model is less precise and only allows the determination of the global stresses, which is insufficient for studying the debonding problem or for a pointwise numerical assessment of the quantities of interest.

In the frequency analysis, we have observed that the system response, in particular for the first resonance peaks, occurs in a frequency band affecting only the metallic cantilever dynamics. On the other hand, in the analysis of the piezoelectric plate submitted to alternating fields, we have shown how the electric resonance frequencies (in the kilohertz range) are much greater than those of interest for the studied system (of some tens of hertz). We conclude that, if the plates were of the same magnitude and on a miniaturized scale, interactions between electrical and mechanical quantities would be stronger, and electrical and mechanical resonances would occur in the same band.

Furthermore, knowledge of very unfavorable resonance peaks in the ordinary working band of the system is crucial for the correct design of the system and to grant the efficiency of

the control and measurement apparatus that uses such electro-mechanical devices. The preliminary tests on the partitioned system were important for the useful conclusion of this work; the initial case study was split into subproblems that are easier to analyze and to test with theoretical and experimental evidence, thereby achieving correct results. The present survey will allow us to synthesize a vibration active control system for the metallic cantilever; further work will address this issue.

ACKNOWLEDGMENT

The authors would like to thank Prof. A. De Simone for his supervision of this work during a visit to the Max Planck Institute for Mathematics in the Sciences, Leipzig, Germany.

REFERENCES

- [1] A. Preumont, "Active Vibration Control," Lecture Notes, Université Libre de Brussel, Brussels, Belgium, 2001.
- [2] J.-M. Breguet, R. Pérez, A. Bergander, C. Schmitt, R. Clavel, and H. Bleuler, "Piezoactuators for motion control from centimeter to nanometer," in *Proc. 2000 IEEE/RSJ Int. Conf. Intelligent Robots Systems*, 2000, pp. 492–497.
- [3] A. F. Vaz and R. Bravo, "Smart piezoelectric film sensors for structural control," *IEEE Trans. Instrum. Meas.*, vol. 53, no. 2, pp. 472–484, Apr. 2004.
- [4] E. Gallasch, D. Rafolt, M. Moser, J. Hindinger, H. Eder, G. Wießpeiner, and T. Kenner, "Instrumentation for assessment of tremor, skin vibrations, and cardiovascular variables in MIR space missions," *IEEE Trans. Biomed. Eng.*, vol. 43, no. 3, pp. 328–333, Mar. 1996.
- [5] S. Bhalla and C. K. Soh, "Structural Impedance Based Damage Diagnosis by Piezo Transducers," *Earthquake Engineering and Structural Dynamics*, vol. 32, pp. 1897–1916, 2003.
- [6] G. Magro, "Electrostatic force microscopy on polycrystalline ferroelectric films," Ph.D. dissertation, Univ. Catania, Catania, Italy, 2000. In Italian.
- [7] S. Tawara, T. Goto, and K. Mitsui, "Miniature tilting mechanism using piezoelectric actuators," *Proc. Int. Soc. Optical Engineering*, vol. 2593, pp. 71–78, 1995.
- [8] D. Sun, L. Tong, and N. Atluri, "Effects of piezoelectric sensor/actuator debonding on vibration control of smart beams," *Int. J. Solids Structures*, vol. 38, no. 50–51, pp. 9033–9051, Dec. 2001.
- [9] J. Holnicki-Szulc and Z. Marzec, "New Technique of Vibration Control," Lecture Notes, Institute of Fundamental Technological Research, Polish Academy Sciences, Warsaw, Poland, 2001.
- [10] R. L. Goldberg, M. J. Jurgens, D. M. Mills, C. S. Henriquez, D. Vaughan, and S. W. Smith, "Modeling of piezoelectric multilayer ceramics using finite element analysis," *IEEE Trans. Ultrason., Ferroelectr., Freq. Control*, vol. 44, no. 6, pp. 1204–1214, Nov. 1997.

- [11] A. Tatone, E. Silverii, and G. Rotoli, "Oscillations of a metallic lamina coupled with a piezoelectric lamina," in *Proc. Como: AIMETA*, Oct. 4–6, 1999, pp. 1–14. In Italian.
- [12] A. Faria Vaz, "Composite modeling of flexible structures with bonded piezoelectric film actuators and sensors," *IEEE Trans. Instrum. Meas.*, vol. 47, no. 2, pp. 513–520, Apr. 1998.
- [13] S. Leleu, H. Abou-Kandil, and Y. Bonnassieux, "Piezoelectric actuators and sensors location for active control of flexible structures," *IEEE Trans. Instrum. Meas.*, vol. 40, no. 6, pp. 1577–1582, Dec. 2001.
- [14] A. Iula, N. Lamberti, and M. Pappalardo, "An approximated 3-D model of cylinder-shaped piezoceramic elements for transducer design," *IEEE Trans. Ultrason., Ferroelectr., Freq. Control*, vol. 45, no. 4, pp. 1056–1064, Jul. 1998.
- [15] N. Lamberti and M. Pappalardo, "A general approximated two-dimensional model for piezoelectric array elements," *IEEE Trans. Ultrason., Ferroelectr., Freq. Control*, vol. 42, no. 2, pp. 243–252, Mar. 1995.
- [16] L. V. Azàroff and J. J. Brophy, *Electronic Processes in Materials*. New York: McGraw-Hill, 1963.
- [17] A. Carpinteri, *Structural Mechanics—A Unified Approach*. Oxford: Chapman & Hall, 1997.
- [18] M. E. Gurtin, *An Introduction to Continuum Mechanics*. New York: Academic, 1981.
- [19] T. Ikeda, *Fundamentals of Piezoelectricity*. New York: Oxford University Press, 1990.
- [20] *IEEE Std 176-1987 IEEE Standard on Piezoelectricity*, 1987.
- [21] I. S. Sokolnikoff, *Mathematical Theory of Elasticity*. New York: McGraw-Hill, 1956.
- [22] W. Voigt, *Lehrbuch der Kristallphysik (Trad: Textbook on Crystal Physics)*. Leipzig, Germany: Teubner-Verlag, 1928. In German.
- [23] ACX QuickPack Devices Descriptions and Specifications (2004). [Online]. Available: <http://www.mide.com/quickpack/qp25n.html>
- [24] A. A. Shabana, *Theory of Vibration—An Introduction*, 2nd ed. Berlin, Germany: Springer, 1996.
- [25] K. J. Bathe, *Finite Element Procedures in Engineering Analysis*. Boston, MA: Prentice-Hall, 1985.
- [26] A. Vv., *Abaqus/Standard—User's Manual, Version 6.2. Hibbit*. Providence, RI: Karlsson and Sorensen Inc., 2001.



Luca Dalessandro (S'02) was born in Bari, Italy, on April 29, 1978. He received the M.Sc. degree in electrical engineering with first class honors from the Politecnico di Bari, Bari, Italy, in 2002. He is currently pursuing the Ph.D. degree at the Swiss Federal Institute of Technology (ETH), Zurich, Switzerland, at its Power Electronic Systems Laboratory (PES).

From 2001 to 2002, he was a Researcher at the Max Planck Institute for Mathematics in the Sciences (MPI-MIS), Leipzig, Germany. His research interests include ac-dc power conversion, electromagnetics, high-performance current sensors, EMC, electromechanical systems modeling and control, and piezoelectricity.

Mr. Dalessandro is a Registered Professional Engineer in Italy.



Daniele Rosato (S'02) was born in Mesagne, Brindisi, Italy, in 1977. He received the M.Sc. degree in electrical engineering with honors from the Politecnico di Bari, Bari, Italy, in 2002 and the M.Sc. degree in computational mechanics of materials and structures with honors from the University of Stuttgart, Stuttgart, Germany, in 2005. He is currently pursuing the Ph.D. degree at the Politecnico di Bari in the Electronic and Electrical Engineering Department (DEE).

From September 2001 to 2003, he was a Visitor Researcher at the Max Planck Institute for Mathematics in the Sciences (MPI-MIS), Leipzig, Germany. He is currently also a Research Associate and COMMAS Course Director at the Institute of Applied Mechanics of the University of Stuttgart. His research interests include electrotechnology, electromechanics, and crystal plasticity.